Open bottom and charm production at ATLAS

M F Watson for the ATLAS Collaboration
School of Physics and Astronomy, University of Birmingham, Edgbaston, Birmingham, B15 2TT, UK; supported by a Royal Society Dorothy Hodgkin Fellowship.

1 Introduction

Results are presented for identified D and B mesons and b-jets, using data collected in 2010 by the ATLAS detector. The most important components of the detector for these analyses are the inner tracking detector and muon system, covering $|\eta| < 2.5$ and $|\eta| < 2.7$, respectively. Events are triggered with minimum bias, muon or jet triggers, depending on the channel under consideration [1]–[6].

2 D meson cross-sections

Charmed hadrons are produced in the fragmentation of charm or bottom quarks, and are identified in the decay modes $\mathrm{D}^{*+} \to \mathrm{D}^0\pi_s^+ \to (\mathrm{K}^-\pi^+)\pi_s^+$, $\mathrm{D}^+ \to \mathrm{K}^-\pi^+\pi^+$ and $\mathrm{D}_s^+ \to \phi\pi^+ \to (\mathrm{K}^-\mathrm{K}^+)\pi^+$, by considering all three-track combinations with suitable kinematic cuts, e.g p_T and $|\eta|$ of the tracks and $\mathrm{D}^{(*)}$ [1]. The reconstructed mass distributions are fitted to extract the number of D meson candidates, from which total cross-sections and differential cross-sections in p_T and $|\eta|$ are extracted. The cross-sections in the kinematic range $p_\mathrm{T}(D^{(*)}) > 3.5$ GeV and $|\eta(D^{(*)})| > 2.1$ are

$$\begin{aligned}
\sigma^{vis}(D^{*\pm}) &= 285 \pm 16(\mathrm{stat.})^{+32}_{-27}(\mathrm{syst.}) \pm 31(\mathrm{lum.}) \pm 4(\mathrm{br.})\ \mu\mathrm{b} \\
\sigma^{vis}(D^{\pm}) &= 238 \pm 13(\mathrm{stat.})^{+35}_{-23}(\mathrm{syst.}) \pm 26(\mathrm{lum.}) \pm 10(\mathrm{br.})\ \mu\mathrm{b} \\
\sigma^{vis}(D_s^{*\pm}) &= 168 \pm 34(\mathrm{stat.})^{+27}_{-25}(\mathrm{syst.}) \pm 18(\mathrm{lum.}) \pm 10(\mathrm{br.})\ \mu\mathrm{b},
\end{aligned}$$

where the systematic uncertainties include contributions from track reconstruction (material description), D meson selection, model dependence, signal fits, luminosity and branching ratios. Figure 1 illustrates the differential cross-sections for $\mathrm{D}^{*\pm}$, in which the data are seen to lie above the NLO predictions, but within the large theoretical (scale) uncertainties.

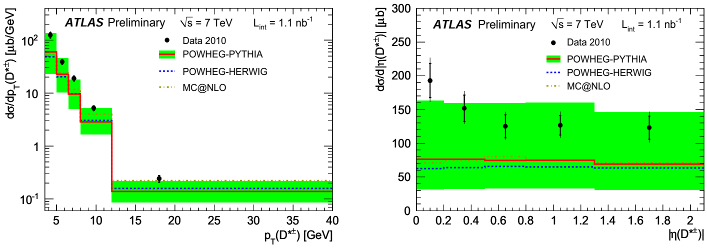

Figure 1: $D^{*\pm}$ differential cross-sections as a function of p_T and $|\eta|$.

3 Exclusive B meson reconstruction

B mesons are reconstructed in the exclusive decay modes $B \to J/\psi + X$, where J/ψ decays to $\mu^+\mu^-$ [2, 3]. Each J/ψ candidate must contain at least one "combined" muon, for which an inner detector track is matched to a track in the muon system.

In order to reconstruct the decay mode $B^\pm \to J/\psi(\mu^+\mu^-)K^\pm$ [2], the muon tracks and an additional track are fitted to a common vertex, with a J/ψ mass constraint for the $\mu^+\mu^-$ and the kaon mass assigned to the third track. The resulting $m_{J/\psi K^\pm}$ mass distribution is enhanced with a transverse decay length cut and is fitted with an unbinned maximum likelihood fit (Gaussian signal and linear background) to extract the $B^\pm$ mass and number of candidates, as seen in Figure 2. The fitted mass is consistent with expectation, and is independent of the B meson charge.

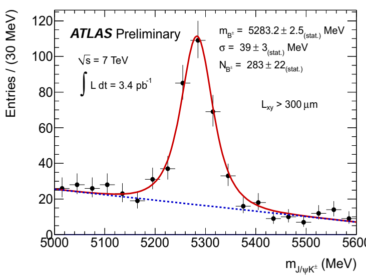

Figure 2: Mass fit for $B^\pm \to J/\psi K^\pm$.

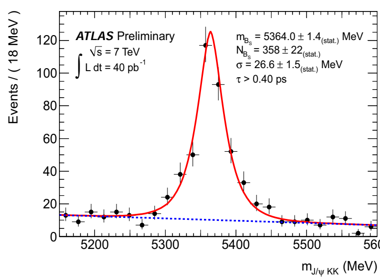

Figure 3: Mass fit for $B_s^0 \to J/\psi\phi$.

A similar analysis is performed for the channels $B_d^0 \to J/\psi K^{*0}$ and $B_s^0 \to J/\psi\phi$ [3]. Two additional tracks are combined with the J/ψ in a four-track fit, assuming the decays $K^{*0} \to K^+\pi^-$ or $\phi \to K^+K^-$. Cuts are applied to $M(\phi)$ or $M(K^{*0})$ and the signal is enhanced with a requirement on the decay time of the fitted secondary vertex. Figure 3 illustrates the observation of $B_s^0 \to J/\psi\phi$ and the maximum likelihood fit to the reconstructed mass. The fitted B_d^0 and B_s^0 masses, both with and without decay time cuts, are consistent with expectation.

4 B jet cross-sections

An enriched sample of jets containing B hadrons ("b-jets") can be obtained by requiring a displaced secondary vertex in the jet [4, 6]. Jets are reconstructed using the anti-k_t algorithm with a cone size $R = 0.4$, then the secondary vertex (SV0) algorithm attempts to find an inclusive vertex with tracks associated to the jet, using an iterative procedure. Secondary vertices are selected with a cut on the decay length significance, relative to the primary event vertex. The b-jet fraction in a sample of tagged jets is obtained from a binned likelihood fit to the vertex mass distribution, using Monte Carlo templates. The fits are performed in bins of jet p_T and rapidity, from which the differential b-jet cross-section can be measured. Efficiency corrections are evaluated with a soft muon tagging procedure, and bin-by-bin corrections for detector effects are applied. In events containing two tagged jets, the dijet cross-section is obtained from template fits to the sum of vertex masses. The systematic uncertainties on both cross-sections are dominated by the b-jet energy scale, and the efficiency and purity of b-jet tagging.

Figure 4 illustrates the differential cross-sections and compares them to Monte Carlo predictions. PYTHIA, which includes leading order and leading logarithm terms, is found to describe the shapes but not the normalisation, while the next-to-leading order predictions of POWHEG show a steeper drop with p_T than in data. The POWHEG dijet cross-section lies above the measured values.

An alternative measurement of the b-jet cross-section uses soft muons to tag an enriched sample of b-jets [5, 6]. Muons within a cone $\Delta R < 0.4$ from the jet axis are considered, and the distribution of muon momentum relative to the jet axis, p_T^{rel}, is fitted using templates. The b-jet fraction obtained in the fits is used to measure the differential cross-section as a function of jet p_T; see Figure 5. This measurement of the cross-section is consistent within uncertainties with the secondary vertex measurement, and with the predictions of POWHEG.

References

[1] ATLAS Collaboration, ATLAS-CONF-2011-017, 12 March 2011, available at https://twiki.cern.ch/twiki/bin/view/AtlasPublic.

[2] ATLAS Collaboration, ATLAS-CONF-2010-098, 16 November 2010.

[3] ATLAS Collaboration, ATLAS-CONF-2011-050, 1 April 2011.

[4] ATLAS Collaboration, ATLAS-CONF-2011-056, 4 April 2011.

[5] ATLAS Collaboration, ATLAS-CONF-2011-057, 11 April 2011.

[6] References [4] and [5] have been updated and combined in "Measurement of the inclusive and dijet cross-sections of b-jets in pp collisions at $\sqrt{s} = 7$ TeV with the ATLAS detector", arXiv:1109.6833 [hep-ex], submitted to EPJC (Sept. 2011).

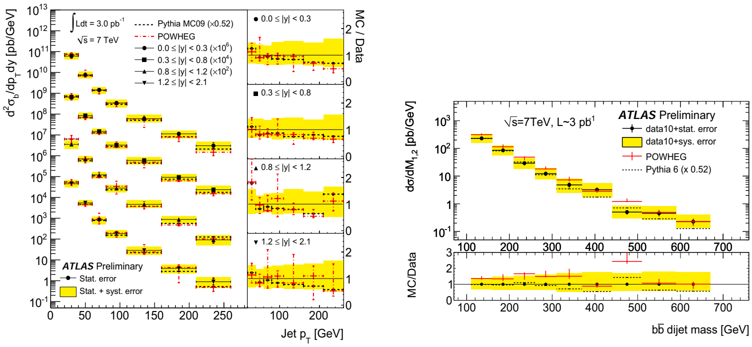

Figure 4: b-jet cross-section (left) and $b\bar{b}$-dijet cross-section (right). The PYTHIA predictions are scaled by 0.52.

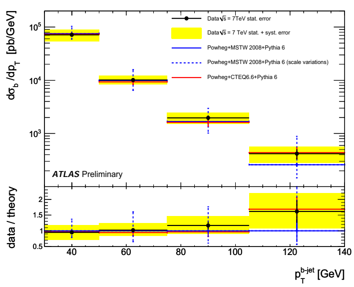

Figure 5: b-jet cross-section using the p_T^{rel} method.